Free energy landscape analysis of two-dimensional dipolar solvent model at temperatures below and above the rotational freezing point

Yohichi Suzuki[a] and Yoshitaka Tanimura
Department of Chemistry, Kyoto University, Oiwakecho, Kitashirakawa, Sakyoku, Kyoto 606-8502, Japan

(Received 28 November 2005; accepted 30 January 2006; published online 27 March 2006)

Ionic solvation in a polar solvent is modeled by a central charge surrounded by dipolar molecules posted on two-dimensional distorted lattice sites with simple rotational dynamics. Density of states is calculated by applying the Wang-Landau algorithm to both the energy and polarization states. The free energy landscapes of solvent molecules as a function of polarization are depicted to explore the competition between the thermal fluctuation and solvation energy. Without a central charge, for temperatures higher than the energy scale of the dipole-dipole interactions, the energy landscape for the small polarization region exhibits a parabolic shape as predicted by Marcus [Rev. Mod. Phys. **65**, 599 (1993)] for electron transfer reaction, while there is an additional quartic contribution to the landscape for the large polarization region. When the temperature drops, the simulated free energy landscapes are no longer smooth due to the presence of multiple local minima arising from the frustrated interaction among the dipoles. The parabolic contribution becomes negligible and the energy landscape becomes quartic in shape. For a strong central charge, the energy landscape exhibits an asymmetric profile due to the contributions of linear and cubic terms that arise from the charge-dipole interactions. © *2006 American Institute of Physics*. [DOI: 10.1063/1.2178785]

I. INTRODUCTION

Ionic solvation is the association of dipolar or ionic solvent molecules with ions of a solute.[1] Solvation plays an important role in many chemical processes in condensed phases such as electron and charge transfer reactions.[2] Complex dipolar interactions among solvent molecules provide the energy fluctuation which is necessary for thermally activated processes. To explore a role of solvation, one possible theoretical approach is to perform full molecular dynamics (MD) simulations by placing the charge in a collection of explicit solvent molecules. To have a fairly complete view of the solvent effect, one has to make an ensemble average over all possible trajectories of molecular motions. This is numerically very difficult besides a high temperature case,[3] since the solvent molecules have too many degrees of freedom and there are too many local minima in the free energy landscape at low temperatures. Despite of the complexity of the system, however, there is still a possibility to explain a role of solvent using a single macroscopic variable. For example, Marcus introduced a free energy landscape as a function of a macroscopic variable representing the collective nature of the solvent molecules. The solvent is treated as a homogeneous dielectric continuum and the free energy landscape is expressed as a quadratic function of the solvent polarization, which is adopted as the reaction coordinate for representing rearrangements of the solvent environment. Electron transfer rates are then evaluated in terms of the free energy landscapes for solvated reactants and products. The advantage of analyzing the system by means of free energy landscape is on the inclusion of entropic contributions upon the possible paths of chemical processes. For example, in a case of electron transfer (ET) or charge transfer (CT) problem,[4–7] a reaction rate may be calculated by averaging over all the possible reaction paths with relevant statistical weight, since there are almost infinite numbers of reaction paths due to so many degrees of freedom that arise from the solvent states. This procedure is almost impossible to carry out except for the high temperature case. The success of the Marcus theory indicates that introducing a free energy landscape is indeed an effective way to describe the reaction processes at least above the freezing temperature.

Since the macroscopic variable may not be sensitive to the microscopic details of the interactions, this suggests that we may employ a simple model to gain insight into a role of ionic solvation. For example, if we separate the rotational and translational degrees of freedom of solvent molecules, we can greatly simplify the statistical analysis and facilitate the construction of reliable energy landscapes at low temperatures.

Several studies based on such a model approach were developed to study dynamical aspects of solvation at high temperature. For example, the Brownian dipolar lattice model,[8,9] which consists of point dipoles fixed on a simple cubic lattice, and the self-consistent continuum model,[10] which describes the rotational motion of a permanent dipole in a spherical Onsager cavity, were used to investigate dielectric relaxation. Papazyan and Maroncelli introduced an ion in a Brownian dipole lattice to study ionic solvation.[11] They performed a numerical simulation of the system and obtained a characterization of the static and dynamic aspects of ionic solvation. Several theories for solvation dynamics were developed[12,13] and compared with computer simulations.[14–16] These models were sufficiently simple to

[a]Electronic mail: yohichi@kuchem.kyoto-u.ac.jp

enable dynamical simulations, but, they still contain too many degrees of freedom to calculate free energy landscapes as a function of polarization, especially at low temperature. For this purpose, we take a minimalist model approach originally proposed by Onuchic and Wolynes to study glassy behavior of solvent molecules in ET or CT reactions.[17] In this approach, ionic solvation in a polar solvent is modeled by a central charge surrounded by dipolar molecules with rotational dynamics represented by dipoles pointing only in two directions, the inward and outward directions relative to the ion. Using this model Onuchic and Wolynes studied the polarization-dependent thermodynamic phase transition analytically by employing a random energy model (REM) approximation,[18,19] where the interaction energies among the solvent molecules were assumed to have a Gaussian distribution independent of the microscopic details of the molecular interactions. It has been shown that, for different magnitudes of polarization, the behavior of the system can be classified into two regions: one is a normal diffusive region, where the linear response picture of the Born-Marcus theory is applicable, and the other is a glassy region, where the dynamics are expected to be very slow. Note that a similar approach was also applied for protein folding problem by Bryngelson and Wolynes.[20] The Onuchic and Wolynes model was also studied by Leite and Onuchic to investigate phase transitions using Monte Carlo kinetics. In addition to the thermodynamic phase transition, they discussed a dynamical phase transition, where the dynamics of dipoles become slow below some critical temperatures.[21] By utilizing the (mean) first passage time idea, the concept of an equivalent diffusion path was proposed. Tanimura *et al.* extended the initial minimalist model to one which has two-layer solvent molecules and includes all dipole-dipole and charge-dipole interactions explicitly, and found multiple glassy transitions associated with the freezing of the different layers of solvent.[22] Many interesting phenomena have been explored by these studies; the free energy landscape has not been studied except using the REM approximation. This is because there are still too many states to enumerate, despite the fact that the positions of dipoles are fixed and each dipole can point out only inward and outward directions. For 20 molecules, there are $2^{20}\sim$one million states.

Due to advances in computer technology and algorithms, we are now able to explore such free energy landscapes even below the freezing temperature. Our aim is to explore the dynamics of solvent molecules as a function of temperature by means of free energy landscape analysis. As the first step, we calculate the density of states applying the Wang-Landau algorithm to both the energy and polarization states and draw the free energy landscape for above and below the freezing temperature. Here, to represent the system more realistically, we extend the minimalist model to a system of dipoles posted on a two-dimensional square lattice with structural disorder including all charge-dipole and dipole-dipole interactions. Random energy model was used to analyze the simulation results.

The organization of this paper is as follows. In Sec. II, a model composed of a single charge and the dipolar solvent is described. The free energy landscape is introduced as a function of a collective solvent variable. In Sec. III, the Wang-Landau algorithm is introduced to calculate the density of states as a function of energy and polarization. The numerical results are presented in Sec. IV, and Sec. V is devoted to the conclusion.

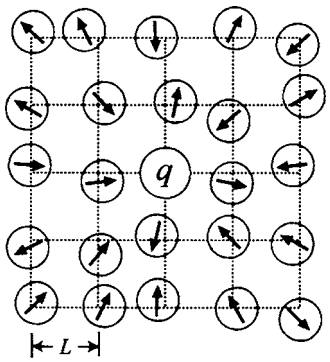

FIG. 1. Schematic view of the solute and solvent model system. A solute molecule is represented by a point charge on the center of two-dimensional square lattice. Solvent molecules are expressed by dipoles located on disordered lattice sites surrounding the central charge. Each dipole is allowed to direct only two directions, toward and opposite to the central charge.

II. SIMULATION MODEL

The minimalist model proposed by Onuchic and Wolynes consisted of a charged cavity and a single shell of solvent molecules represented by dipoles with simple rotational dynamics. These dipoles were allowed to point only two directions, toward and opposite to the charged cavity.[17] Tanimura *et al.* extended the single shell of solvent molecules to two layers. Monte Carlo simulations were carried out on this system including all dipole-dipole and charge-dipole interactions.[22] Here, we post the dipoles on a two-dimensional square lattice having lattice constant L and containing structural disorders (Fig. 1). The position of the jth dipole $\mathbf{r}_j$ can be expressed using a lattice point vector $\mathbf{a}_j$ and displacement vector from the lattice point $\delta\mathbf{a}_j$, i.e., $\mathbf{r}_j=\mathbf{a}_j+\delta\mathbf{a}_j$. The strength and the unit vector specifying the direction of a dipole are μ and $\mathbf{S}_j$, where $\mathbf{S}_j=\mathbf{r}_j/|\mathbf{r}_j|$. If we introduce the sign operator $\sigma_j=\pm 1$, where the sign depends on whether the dipoles are pointing toward or away from the charge, the dipole movement is expressed as $-\mu\sigma_j\mathbf{S}_j$. Thus, the charge-dipole and dipole-dipole interactions are explicitly given by[22]

$$E_{\mathrm{tot}}(\{\sigma_i\}) = -\sum_{i=1}^{N} \xi_i(q)\sigma_i + \sum_{j=2}^{N}\sum_{k=1}^{j-1} J_{jk}\sigma_j\sigma_k, \tag{2.1}$$

where we set

$$\xi_i(q) = -\frac{\mu q}{r_i^2} \tag{2.2}$$

and

$$J_{jk} = \mu^2 \frac{\mathbf{S}_j\cdot\mathbf{S}_k|\mathbf{r}_{jk}|^2 - 3(\mathbf{S}_j\cdot\mathbf{r}_{jk})(\mathbf{S}_k\cdot\mathbf{r}_{jk})}{|\mathbf{r}_{jk}|^5}, \tag{2.3}$$

with $\mathbf{r}_{jk}=\mathbf{r}_j-\mathbf{r}_k$. The system exhibits a glassy behavior at low temperatures because of these complex interactions with

structural disorder. For the units of parameters, we employ values typical of ET or CT systems in polar solvents. Thus, q, μ, and L are chosen to be 0.1 of the electron charge, the unit of Debye, and the unit of 2.1Å, respectively. Adopting such typical units, the energy unit becomes 1.08×10^{-20} J, which is about $2.5k_BT$ at room temperature. Then, simulations are carried out for $\mu=1.85$ and $L=1$ for different q and temperatures. The displacements from the lattice points obey a Gaussian distribution with average $\langle\delta\mathbf{a}_j\rangle=0$ and standard deviation $\sqrt{\langle\delta\mathbf{a}_j^2\rangle}=0.1$. As a collective solvent coordinate, we introduce the total polarization defined by

$$p=n_--n_+, \tag{2.4}$$

where n_+ and n_-, respectively, represent the number of dipoles directed inward to and outward from the charged cavity, and the total number of dipoles is given by

$$N=n_-+n_+. \tag{2.5}$$

We further introduce the average polarization per dipole defined by $x=p/N$. The free energy landscape is then expressed in terms of x and T as

$$\frac{F(x,T)}{N}=-\frac{k_BT}{N}\ln\sum_{\{\sigma_i\}\in x}\exp(-E_{\mathrm{tot}}(\{\sigma_i\})/k_BT), \tag{2.6}$$

where the summation is taken over all configurations for which $x=x(\{\sigma_i\})$. Even in the present model which consists of a charged cavity and 80 dipoles on 9×9 two-dimensional square lattice, there are too many states to enumerate all configurations in this summation. Some procedures for efficiently sampling relevant states therefore are essential in order to construct the free energy landscapes. Our approach is described in the following section.

III. SIMULATION METHOD

The difficulty in evaluating Eq. (2.6) arises from the astronomically large number of states involved in the summation. Fortunately, such a large number of states allow us to employ a statistical treatment. If we obtain a subset of the ensemble that is representative of all of the states in the summation in Eq. (2.6), we may evaluate $F(x,T)$ from the subset. The Monte Carlo method with Metropolis algorithm has been used to generate such representative ensembles, but this approach is time consuming for a glassy system at low temperature, because the trajectory of sampled states generated by the Monte Carlo method is easily trapped in the local energy minima. To overcome this difficulty, Berg and Neuhaus proposed the multicanonical algorithm,[23,24] which has been applied to many problems such as spin glasses, proteins, and polymers.[25–27] The important aspect of this algorithm is the generation of a uniform sampling of configurations in energy space using artificial sampling weights instead of the Boltzmann weights. It means that the algorithm performs a random walk in energy space that allows the system to overcome energy barriers. From a set of sampling data, one can obtain thermodynamic averages at arbitrary temperatures. Furthermore, the calculation of the entropy and the free energy, which are associated with the partition function, is possible. Many researchers have attempted to improve the efficiency of such algorithms.[28,29] Recently an efficient algorithm for estimating the weight factors was developed by Wang and Landau.[30,31] This algorithm consists of two steps: the first step is obtaining the artificial weight factors by recursive updates, which enables us to get flat histogram (uniform sampling data in the energy space), and the second step is generating configurations using such weight factors and calculating physical quantities by reweighting probabilities to conform to the Gibbs ensemble. This algorithm is efficient for evaluating the free energy, but in order to calculate the free energy landscape, which is a function of the polarization per molecule, extension is necessary. We use the two-dimensional Wang-Landau algorithm to obtain the proper weighting factor not only for the energy space but also for the polarization space. This algorithm enables us to obtain the free energy landscape for all possible ranges of the polarization at any temperature.

The outline of the procedure is the following. First, we introduce the weight factor $g(E,x)$ as a function of the energy E and the average polarization per dipole x. The transition probability from (E_1,x_1) to (E_2,x_2) is then defined by

$$p((E_1,x_1)\rightarrow(E_2,x_2))=\min\left[\frac{g(E_1,x_1)}{g(E_2,x_2)},1\right], \tag{3.1}$$

where (E_1,x_1) and (E_2,x_2) refer to states before and after a single dipole is flipped. Next, we introduce the histogram $H(E,x)$ defined by the number of visits made to each state (E,x). If we can make the histogram sufficiently flat using the transition rule (3.1), the density of states $n(E,x)$ will satisfy the following relation at arbitrary (E_1,x_1) and (E_2,x_2):

$$\frac{n(E_1,x_1)}{n(E_2,x_2)}=\frac{g(E_1,x_1)}{g(E_2,x_2)}. \tag{3.2}$$

To obtain a flat histogram, first, we set $g(E,x)=1$ for all possible ranges of energy and polarization. In each time step, if the system attains to the states of energy E and polarization x during the update procedure [Eq. (3.1)], the weight factor is modified as $g(E,x)\rightarrow f_0g(E,x)$, where f_0 is a modification factor set by $f_0=e\cong2.718\,28$. If the transition $(E_1,x_1)\rightarrow(E_2,x_2)$ is rejected, we also modify the factor as $g(E_1,x_1)\rightarrow f_0g(E_1,x_1)$. Iterating this update procedure yields a random walk in energy and polarization space and the modification of weight factors within the accuracy of f_0. When the histogram $H(E,x)$ becomes sufficiently flat, we update the modification factor f_0 as $f_1=\sqrt{f_0}$ and reset the histogram. In practice, it is not easy to obtain a perfectly flat histogram, thus if $H(E,x)$ for all possible E and x attains larger than 80% of the averaged value, $\langle H(E,x)\rangle$, we regard that the histogram is flat. This procedure will be repeated for new modification factor f_i for $i>1$ with $f_i=\sqrt{f_{i-1}}$. The updating of f_i enables us to modify the weight factor more finely. We stop this iteration once $f_i<1.000\,000\,01$. After we obtain the weight factors to satisfy Eq. (3.2), we can normalize the density of states $n(E,x)$ using the condition

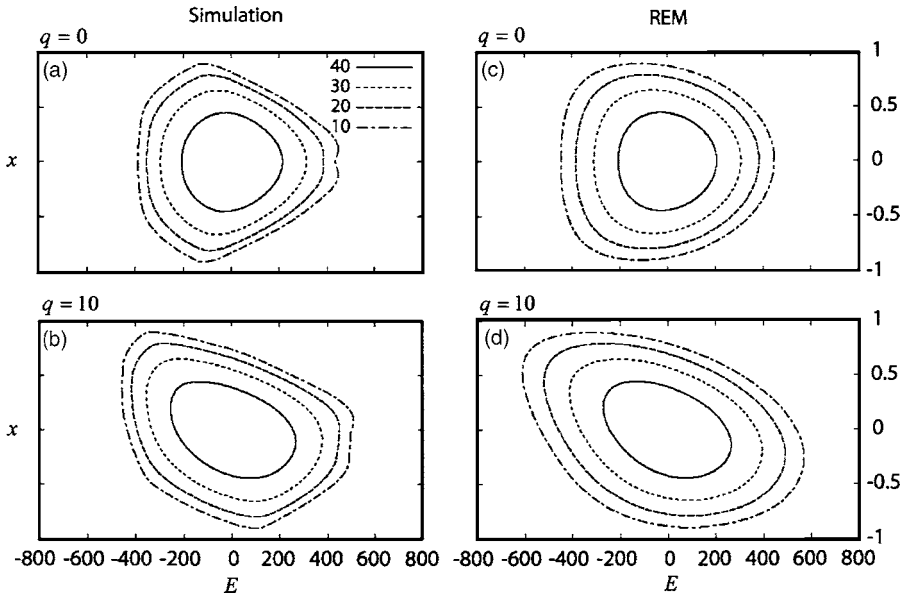

FIG. 2. Counter maps of the logarithms of the density of states are plotted for the cases of (a) no central charge $q=0$ and (b) strong central charge $q=10$. For comparison, the logarithms of the average density of states used in the REM approximation are also plotted as contour maps for the cases of (c) no central charge and (d) strong central charge.

$$\sum_{E,x} n(E,x) = 2^N. \tag{3.3}$$

Substituting Eq. (3.2) into Eq. (3.3) yields

$$n(E,x) = 2^N \frac{g(E,x)}{\Sigma_{E,x} g(E,x)}. \tag{3.4}$$

Finally, from Eq. (2.6), we have the expression of the free energy landscape as

$$\frac{F(T,x)}{N} = -\frac{k_B T}{N} \ln\left(\sum_E n(E,x) \exp\left(-\frac{E}{k_B T} \right) \right). \tag{3.5}$$

In our simulation, we divide the regions of energy (−700 and 700) and polarization (−1 and 1) into 1401 and 81 segments. Since the directions of the dipoles are restricted to point toward and opposite to the central charged cavity, the periodic boundary conditions are not appropriate for our model. To avoid artificial error from the boundary, here we use the open boundary condition. While we study the effect of the central charge upon the surrounding dipoles, we can suppress the influence of boundary dipoles by choosing the large lattice. The validity of the model can be easily checked by changing the lattice size.

IV. DENSITY OF STATES AND FREE ENERGY LANDSCAPE

Following the procedure in the previous section, we have carried out simulations of a system composed of a charged cavity and 80 dipoles on the 9×9 two-dimensional square lattice with $\mu=1.85$ and $L=1$. In order to adjust the lattice size, we repeated the simulations for the 7×7 and 11×11 lattices and we found that the properties of the free energy landscape do not change qualitatively if the size is larger than 7×7. The displacements from the lattice points obeyed a Gaussian distribution with the average $\langle \delta \mathbf{a}_j \rangle = 0$ and the standard deviation $\sqrt{\langle \delta \mathbf{a}_j^2 \rangle} = 0.1$. By using the two-dimensional Wang-Landau algorithm, we obtained the density of states (DOS) as the function of the energy E and the polarization x, $n(x,E)$, for different central charges $q=0$ and 10. For comparison we also evaluated the average DOS, $\langle n(x,E) \rangle$, used in the REM theory, where all dipole-dipole and charge-dipole interactions are assumed to have a random Gaussian distribution function.[17,21] The REM theory assumes the unrealistic interactions among the molecules but this allows us to obtain a handy analytical expression for free energy landscape.

The outline of the REM theory is explained in the Appendix. Note that the theory may not predict the energy landscape properly below the freezing temperature, since a glassy system becomes frozen in low energy states; the free energy landscape has local minima in shape. However, the theory averages over the local minima, thus the landscape is no longer ragged function.

In order to adapt the REM theory to the simulation model, we set the averaged charge-dipole interaction $\bar{\xi}(q) = 0.0$, the dipole-dipole interaction $\bar{J} = -0.05$, and their standard deviations $\Delta\xi^2 = 0.0$ and $\Delta J^2 = 0.91$ for zero central charge $q=0$; and $\bar{\xi}(q) = -2.90$, $\bar{J} = -0.05$, $\Delta\xi^2 = 14.64$, and $\Delta J^2 = 0.91$ for strong central charge $q=10$, respectively.

We plot $\ln n(x,E)$ in Figs. 2(a) and 2(b), and $\ln\langle n(x,E) \rangle$ in Figs. 2(c) and 2(d) as contour maps for $q=0$ and $q=10$, respectively.

In the peak region denoted by the solid lines, both simulation and REM for $q=0$ show symmetrical profiles, whereas (b) and (d) for $q=10$ show unsymmetrical ellipsoidal profiles in the x direction due to the energy difference between the inner and outer directions of dipoles arising from the charge-dipole interaction. For the low energy region $E < -200.0$, the distributions of $\ln\langle n(x,E) \rangle$ are always broader than those of $\ln n(x,E)$. This is because, to adapt to the simulation results, we have overestimated the width of a Gaussian distribution of the interaction energies used in the REM theory. The energy distribution from the simulation, which is not shown here, is characterized by the sum of narrower non-Gaussian peaks.

The free energy landscape (FEL) is calculated from Eq. (3.5). For comparison we have also evaluated the FEL for the REM case from (see Appendix)

$$F_{\mathrm{REM}}(x,T)/N = \begin{cases} \frac{1}{N}\left(\bar{E}(x) - \frac{\Delta E^2}{2T} - TS^*(Nx)\right) & \text{for } T > T_c(x) \quad (4.1) \\ \frac{1}{N}(\bar{E}(x) - \Delta E(2S^*(Nx))^{1/2}) & \text{for } T \leqslant T_c(x), \quad (4.2) \end{cases}$$

with

$$S^*(Nx) = N\left[-\left(\frac{1+x}{2}\right)\ln\left(\frac{1+x}{2}\right) - \left(\frac{1-x}{2}\right)\ln\left(\frac{1-x}{2}\right)\right], \tag{4.3}$$

by using the same parameters for the DOS calculation. Here the average solvation energy at polarization x and the standard deviation of the solvation energy are expressed as $\bar{E}(x)$ and ΔE. The FELs have two types of form above and below a polarization-dependent phase transition temperature $T_c(x)$. Figures 3(a)–3(c) show the FELs from the simulations (solid line) and the REM (dashed line) for zero central charge $q=0$. Figures 3(d)–3(f) show the corresponding data for a strong central charge $q=10$. These temperatures are $T=20$, 7, and 1. The dotted lines in Fig. 3 represent the fourth-order polynomial fits $F(x)=\Sigma_{j=1}^{4}a_j x^j$ in addition to a constant term.

The high temperature case $T=20$ is shown in Figs. 3(a) and 3(d). This temperature satisfies $T>T_c(x)$ for all ranges of x and the REM results denoted by the dashed lines are calculated only from Eq. (4.1). The FEL from the simulation exhibits a similar profile as the REM results. Both curves are parabolic for small $|x|$ as predicted by the Born-Marcus theory,[1] but the curvature increases for large $|x|$ due to the entropic contribution. In the REM case, this contribution arises from $TS^*(Nx)$ in Eq. (4.1), where $S^*(Nx)$ is a logarithmic function of x. To illustrate the effects of the entropic contribution, we expand $F_{\mathrm{REM}}(x,T)/N$ in Eqs. (4.1) and (4.2) for small x as

$$F_{\mathrm{REM}}(x,T)/N = \begin{cases} -\left(\frac{\Delta E^2}{2TN} + T\ln 2\right) + x\bar{\xi}(q) + x^2\left(z\bar{J} + \frac{T}{2}\right) + x^4\left(\frac{T}{12}\right) + \cdots, & T > T_c(x) \quad (4.4) \\ -\Delta E\sqrt{\frac{2}{N}\ln 2} + x\bar{\xi}(q) + x^2\left(z\bar{J} + \frac{\Delta E}{4}\sqrt{\frac{2}{N\ln 2}}\right) + x^4\left(\frac{\Delta E(3+4\ln 2)}{96(\ln 2)^{3/2}}\sqrt{\frac{2}{N}}\right) + \cdots, & T \leqslant T_c(x), \quad (4.5) \end{cases}$$

where z is the average number of dipoles interacting with each single dipole.

As can be seen from Eq. (4.4), when the temperature becomes high, the contributions of the second-order coefficient as well as of the fourth-order contribution become large. When a central charge is present, the dipoles tend to point outward to decrease the energy and the term proportional to x in Eq. (4.4) also plays a role in the REM case; the minimum point of landscape shifts to the positive direction. In the simulation case, there is also cubic contribution to FEL. The fitting function now involves all terms as $F(x)=\Sigma_{j=1}^{4}a_j x^j$. The lack of the cubic term in the REM case is due to the oversimplification of charge-dipole interactions. In the simulation model, the intensity of the charge-dipole interaction changes with the location of dipoles, which makes the free energy a complex function of the polarization. In contrast the REM theory assumes a spatially uniform interaction which makes the free energy a linear function of polarization.

Figures 2(b) and 2(e) are for the intermediate temperature $T=7$. The REM results in the region of $|x|<0.8$ for Fig. 2(b) and $|x|<0.6$ for Fig. 2(e) are calculated from Eq. (4.1) to satisfy $T>T_c(x)$, whereas those in the remaining regions are calculated from Eq. (4.2). The FELs calculated by the REM are broader than the simulated ones, especially in the region around $x=1$ and $x=-1$. As explained in Fig. 2, this can be explained by the fact that a profile of the lower part of average DOS is always broader because of the overestimation of energy distribution. In the same manner as in the high temperature case, the free energy landscape can be well fitted by a polynomial function. As this lower temperature, the fourth-order contribution of the fitting curves becomes large as is illustrated by the REM theory. For the fixed parameter $z\bar{J}=-1.8$, the ratio a_4/a_2 in Eq. (4.4) increases with decreasing temperature up to $T=3.6$.

Figures 3(c) and 3(f) show the results for the low temperature case $T=1$. The REM results are calculated from Eq. (4.2), since this temperature satisfies $T\leqslant T_c(x)$ for all ranges of x. At this very low temperature, the simulated FELs are no longer smooth due to the presence of multiple local minima arising from the frustrated interaction among the dipoles. This roughness can be clearly distinguished from the numerical error of the simulations; the error in these calculation is less than the line in Fig. 3.

Notice that the roughness depends upon the disorder of the dipoles. Thus, if we make the ensemble average of the FELs for different configurations of dipoles, this roughness may be smoothed over. On the contrary, the landscape for the REM is smooth even at low temperature, since the REM assumes the smooth Gaussian function for the average DOS.

The profile of the FEL as shown in Fig. 3(c) is expressed by a quartic function $F(x)\approx a_4 x^4$, instead of the parabolic function except for small roughness of lines. On the other hand, in Eq. (4.5), the contribution of the parabolic term

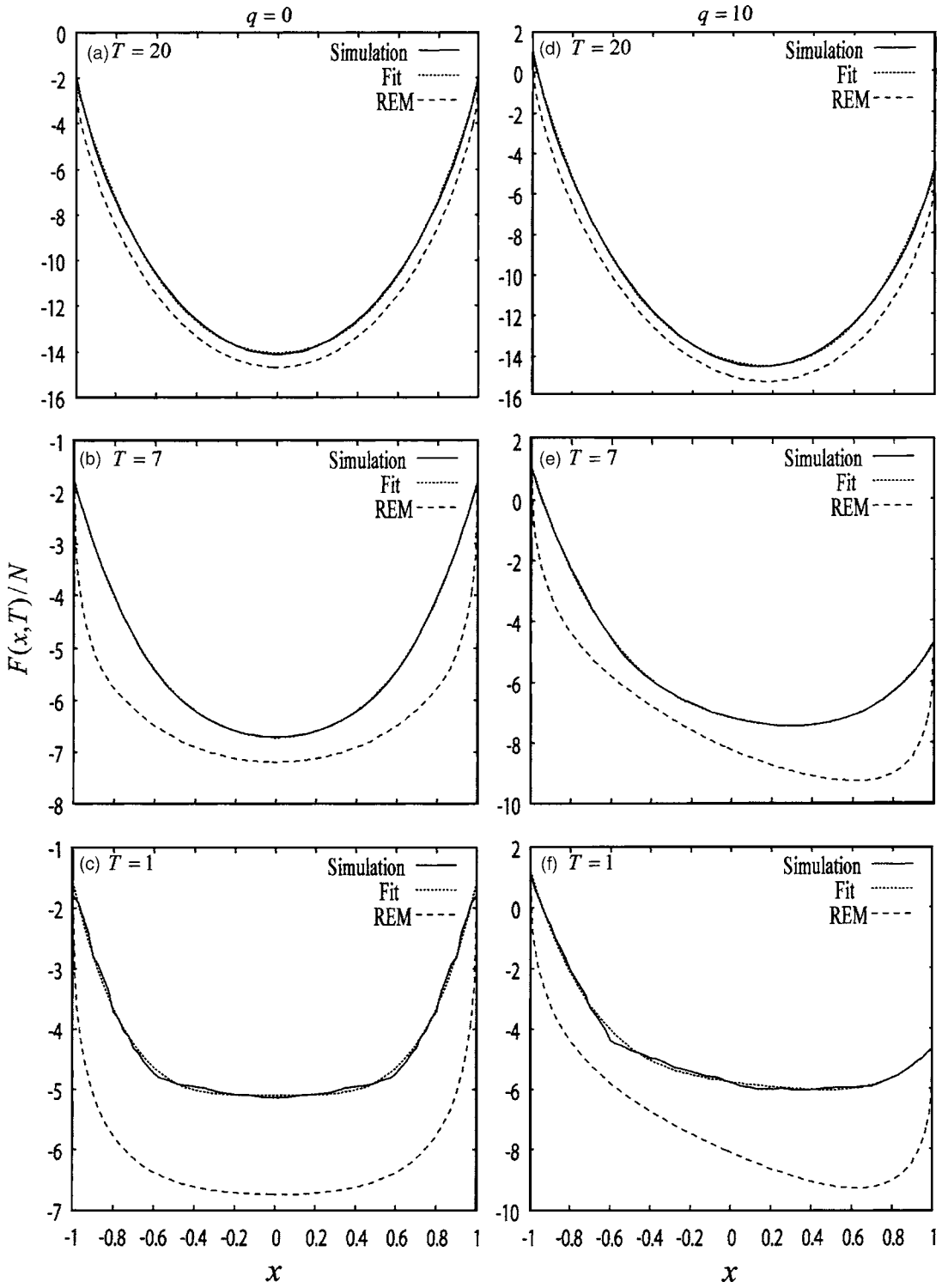

FIG. 3. Free energy landscapes as the function of the polarization in the case of no central charge $q=0$ [(a)–(c)] and strong central charge $q=10$ [(d)–(f)] for different temperatures $T=20$, $T=7$, and $T=1$. The solid, dotted, and dashed lines represent the results of our simulation, fourth-order polynomial fits, and the REM, respectively.

compared with the quartic term is not negligible ($a_2/a_4=0.75$ for $z\bar{J}=-1.8$). Thus the quartic profile of the FEL cannot be explained only by entropic contribution. Since the dipole-dipole interactions are assumed to be Gaussian random variables, complex interactions depending on the position of dipoles are not considered in the REM theory. Moreover the average energy at polarization x is given by parabolic form. The fact that the strong quartic dependence of the FEL is observed at low temperature suggests that the average energy contains quartic term due to the spatial correlation among dipoles.

Figure 3(f) illustrates the energy landscape for a central charge of $q=10$. In addition to the parabolic and quartic contributions of x, the REM case exhibits the linear contribution, i.e., $F(x)\approx a_1x+a_2x^2+a_4x^4$, whereas for the simulation case exhibits the linear and cubic contributions, i.e.,

$F(x) \approx a_1 x + a_2 x^2 + a_3 x^3 + a_4 x^4$. As explained in Fig. 3(d), both the linear and cubic contributions arise from the charge-dipole interaction. Indeed, they appeared even we calculated the FEL for a model without the dipole-dipole interactions (not shown).

V. CONCLUSION

We calculated the free energy landscape as a function of polarization for a two-dimensional charge-dipole lattice model using the Wang-Landau algorithm. To elucidate the entropic contributions to the free energy, we supplemented the calculations using the REM approach by taking the parameters from the simulation model. In the high temperature case without a central charge, the free energy landscapes calculated from the simulation and REM are parabolic in shape for small polarizations, as the Born-Marcus theory predicts. In the large polarization region, both the simulated and REM results also include a small quartic contribution, that arises from the entropic term in the definition of the free energy as pointed out by Onuchic and Wolynes.[17]

For a strong central charge, the free energy landscape becomes asymmetric as a result of charge-dipole interactions. In addition to the quadratic and quartic terms, the free energy landscape is fitted by the linear and cubic terms in the simulation case whereas only by a linear term observed in the REM case, because the REM theory oversimplifies the form of the charge-dipole interactions.

When the temperature decreases, the difference between the numerical and REM results becomes pronounced. This can be explained more clearly when we plot the DOS as a function of both energy and polarization. The REM results exhibit a broader DOS due to the overestimation of the interaction energies chosen to adjust the simulation model to the REM theory. In the low temperature case, the free energy landscape observed in the simulations is no longer smooth. The roughness arises from the inhomogeneous charge-dipole and dipole-dipole interactions and depends upon the positions of the dipoles. Ignoring this roughness, the profile of the free energy landscape is fitted by a polynomial function up to the fourth order of the polarization. As in the high temperature case, the linear and cubic contributions appear when a strong central charge is introduced.

In this paper we have calculated the free energy landscape of a system composed of a charged cavity and dipoles which are restricted to point only two directions. The present model is too simple to describe many important effects involved in solvation dynamics, such as librational motion. Generalization to a realistic model with the large degrees of freedom in three-dimensional space is necessary to explore the universality of our results. Thermal as well as dynamical aspects of such system are important to relate the free energy landscape to real experiments of a relaxation. Future extensions of this work involve studying the relation between thermal and dynamical properties of more realistic systems.

ACKNOWLEDGMENTS

The authors wish to express gratitude to Professor Mark Maroncelli for fruitful discussions. One of the authors (Y.T.) is thankful for the financial support from a Grant-in-Aid for Scientific Research A 15205005 from Japan Society for the Promotion of Science and Morino Science Foundation.

APPENDIX: BRIEF SUMMARY OF RANDOM ENERGY MODEL (REM)

In a framework of the random energy model (REM), all dipole-dipole and charge-dipole interactions are assumed to have a random Gaussian distribution function characterized by the averaged charge-dipole and dipole-dipole interactions $\bar{\xi}(q)$ and $\bar{J}$, and their standard deviations $\Delta\xi$ and ΔJ. The average solvation energy is then given by[17,21]

$$\bar{E}(x) = N[x\bar{\xi}(q) + z\bar{J}x^2], \tag{A1}$$

where z is the average number of dipoles interacting with each single dipole. The standard deviation of the solvation energy is assumed to be independent of x and given by

$$\Delta E^2 = N[\Delta\xi^2 + z\Delta J^2]. \tag{A2}$$

Introducing the probability distribution $g(x,E)$ at polarization x as

$$g(x,E) = \frac{1}{\sqrt{2\pi}\Delta E} \exp\left[-\frac{(E-\bar{E}(x))^2}{2\Delta E^2} \right] \tag{A3}$$

yields an average density of states with polarization x and energy between E and $E+dE$,

$$\langle n(x,E)\rangle = \Omega(Nx) g(x,E) dE, \tag{A4}$$

where

$$\Omega(Nx) = \frac{N!}{n_+! n_-!} = \frac{N!}{[N(1-x)/2]![N(1+x)/2]!} \tag{A5}$$

is the total number of states with polarization x. For $\langle n(x,E)\rangle \gg 1$, one can approximate $\langle \ln n(x,E)\rangle$ by $\ln\langle n(x,E)\rangle$, and the entropy can be written by

$$\begin{aligned} S(x,E) &\approx \ln\langle n(x,E)\rangle \\ &\approx \ln \Omega(Nx) - \frac{(E-\bar{E}(x))^2}{2\Delta E^2}. \end{aligned} \tag{A6}$$

The above approximation is not valid below the critical energy,

$$E_c(x) = \bar{E}(x) - \Delta E(2 \ln \Omega(Nx))^{1/2}, \tag{A7}$$

since the entropy becomes negative. Therefore we set $S(x,E)=0$ for $E<E_c(x)$. This result indicates a polarization-dependent phase transition at the temperature

$$T_c(x) = \frac{\Delta E}{[2S^*(Nx)]^{1/2}}, \tag{A8}$$

where the configuration entropy $S^*(Nx)$ is given by $S^*(Nx) = \log(\Omega(Nx))$. In the large N limit, the configuration entropy becomes

$$S^*(Nx) = N\left[-\left(\frac{1+x}{2}\right)\ln\left(\frac{1+x}{2}\right) - \left(\frac{1-x}{2}\right)\ln\left(\frac{1-x}{2}\right)\right], \tag{A9}$$

with the aid of Stirling's formula. Then the free energy landscape for the REM approximation is expressed as

$$F_{\mathrm{REM}}(x,T)/N = \begin{cases} \dfrac{1}{N}\left(\bar{E}(x) - \dfrac{\Delta E^2}{2T} - TS^*(Nx)\right) & \text{for } T > T_c(x) \quad \text{(A10)} \\ \dfrac{1}{N}(\bar{E}(x) - \Delta E(2S^*(Nx))^{1/2}) & \text{for } T \leqslant T_c(x). \quad \text{(A11)} \end{cases}$$

To determine the average number of interacting dipoles z for dipole-dipole interactions, which affects long range, we use the following condition:

$$F(1,T)/N = F_{\mathrm{REM}}(1,T)/N = \bar{E}(1)/N. \tag{A12}$$

Note that, in Eq. (A12), we always use the free energy for $T \leqslant T_c(x)$ because $T_c(x)$ becomes infinite when $x \to 1$.

[1] R. A. Marcus, Rev. Mod. Phys. **65**, 599 (1993).
[2] F. Hirata, *Molecular Theory of Solvation* (Kluwer Academic, Dordrecht, 2003).
[3] I. Benjamin, P. F. Barbara, B. J. Gertner, and J. T. Hynes, J. Phys. Chem. **99**, 7557 (1995).
[4] J. Ulstrup and J. Jortner, J. Chem. Phys. **63**, 4358 (1975).
[5] M. Tachiya, J. Phys. Chem. **93**, 7050 (1989).
[6] K. Ando and S. Kato, J. Chem. Phys. **95**, 5966 (1991).
[7] A. Yoshimori, T. Kakitani, Y. Enomoto, and N. Mataga, J. Phys. Chem. **93**, 8316 (1989).
[8] R. Zwanzig, J. Chem. Phys. **38**, 2766 (1963).
[9] H.-X. Zhou and B. Bagchi, J. Chem. Phys. **97**, 3610 (1992).
[10] T.-W. Nee and R. Zwanzig, J. Chem. Phys. **52**, 6353 (1970).
[11] A. Papazyan and M. Maroncelli, J. Chem. Phys. **95**, 9219 (1991).
[12] P. G. Wolynes, J. Chem. Phys. **86**, 5133 (1987).
[13] L. E. Fried and S. Mukamel, J. Chem. Phys. **93**, 932 (1990).
[14] S. S. Komath and B. Bagchi, J. Chem. Phys. **98**, 8987 (1993).
[15] H.-X. Zhou, B. Bagchi, A. Papazyan, and M. Maroncelli, J. Chem. Phys. **97**, 9311 (1992).
[16] A. Papazyan and M. Maroncelli, J. Chem. Phys. **102**, 2888 (1995).
[17] J. N. Onuchic and P. G. Wolynes, J. Chem. Phys. **89**, 2218 (1993).
[18] B. Derrida, Phys. Rev. B **24**, 2613 (1981).
[19] B. Derrida, Phys. Rev. Lett. **45**, 79 (1980).
[20] J. D. Bryngelson and P. G. Wolynes, J. Phys. Chem. **93**, 6902 (1989).
[21] V. B. P. Leite and J. N. Onuchic, J. Phys. Chem. **100**, 7680 (1996).
[22] Y. Tanimura, V. B. P. Leite, and J. N. Onuchic, J. Chem. Phys. **117**, 2172 (2002).
[23] B. A. Berg and T. Neuhaus, Phys. Lett. B **267**, 249 (1991).
[24] B. A. Berg and T. Neuhaus, Phys. Rev. Lett. **68**, 9 (1992).
[25] B. A. Berg and T. Celik, Phys. Rev. Lett. **69**, 2292 (1992).
[26] U. H. E. Hansmann and Y. Okamoto, J. Comput. Chem. **14**, 1333 (1993).
[27] N. Urakami and M. Takasu, J. Phys. Soc. Jpn. **65**, 2694 (1996).
[28] A. Mitsutake, Y. Sugita, and Y. Okamoto, Biopolymers **60**, 96 (2001).
[29] Y. Okamoto, J. Mol. Graphics Modell. **22**, 425 (2004).
[30] F. Wang and D. P. Landau, Phys. Rev. Lett. **86**, 2050 (2001).
[31] F. Wang and D. P. Landau, Phys. Rev. E **64**, 056101 (2001).